Journal of Cleaner Production 238 (2019) 117862

Contents lists available at ScienceDirect

Journal of Cleaner Production

journal homepage: www.elsevier.com/locate/jclepro

Pollutants emitted from typical Chinese vessels: Potential contributions to ozone and secondary organic aerosols

Di Wu [a], Xiang Ding [a], Qing Li [a, b, **], Jianfeng Sun [a], Cheng Huang [c], Lan Yao [a], Xinming Wang [d], Xingnan Ye [a, b], Yingjun Chen [a], Hong He [e], Jianmin Chen [a, b, e, *]

[a] Shanghai Key Laboratory of Atmospheric Particle Pollution and Prevention, Department of Environmental Science and Engineering, Institute of Atmospheric Sciences, Fudan University, Shanghai, 200433, China
[b] Shanghai Institute of Eco-Chongming (SIEC), No. 3663 Northern Zhongshan Road, Shanghai, 200062, China
[c] State Environmental Protection Key Laboratory of Formation and Prevention of Urban Air Pollution Complex, Shanghai Academy of Environmental Sciences, Shanghai, 200233, China
[d] State Key Laboratory of Organic Geochemistry, Guangzhou Institute of Geochemistry, Chinese Academy of Sciences, Guangzhou, 510640, China
[e] Center for Excellence in Regional Atmospheric Environment, Institute of Urban Environment, Chinese Academy of Sciences, Xiamen, 361021, China

ARTICLE INFO

Article history:
Received 5 May 2019
Received in revised form
3 July 2019
Accepted 31 July 2019
Available online 1 August 2019

Handling Editor: Cecilia Maria Villas Bôas de Almeida

Keywords:
Ship emissions
Particulate matter
VOC species
Secondary organic aerosol
Ozone formation

ABSTRACT

Pollutants emitted from ships have adverse effects on the atmospheric environment. In this study, the atmospheric impact of gaseous and particulate pollutants emitted in the exhaust of typical ships was estimated based on real-world measurements obtained under conditions of various engine speeds and fuel types. The results showed that $PM_{2.5}$ emission factors (EFs) ranged between 0.38 ± 0.01 and 1.05 ± 0.04 g/kg fuel, and tended to increase with engine speed. The EFs of volatile organic compounds (VOCs; including 57 species), which varied between 63 ± 4 and 156 ± 6 mg/kg fuel at different engine speeds, were determined largely via the modified combustion efficiency. The ozone formation potential (OFP), dominated by alkanes and aromatics, was between 0.33 ± 0.01 and 0.83 ± 0.05 g O_3/kg fuel. Secondary organic aerosol formation potential (SOAFP), dominated primarily by aromatics, varied between 2.7 ± 0.1 and 8.7 ± 0.7 mg SOA/kg fuel. Switching from heavy fuel oil to diesel oil significantly reduced pollutant emissions with the exception of NO_x. Reductions in the EFs of VOCs, $PM_{2.5}$, and total suspended particles were 67%, 42%, and 66%, respectively. The average fuel-mass-based EFs of OFP and SOAFP from ship emissions were ~2.3- and ~2.6-fold greater than those exhausted from on-road diesel vehicles, respectively, indicating that ship emissions could be an important source for ground-level ozone and organic aerosol formation, particularly in coastal regions. The results suggest that emission abatement technologies should be applied to marine diesel engines and stringent regulations on VOC species, particularly aromatics, should be imposed to improve regional air quality.

1. Introduction

Pollutant emissions from ships have recently received increasing attention because of their significant negative effects on the atmospheric environment and human health (Eyring et al., 2010; Lin et al., 2018). Gas-phase pollutants such as nitrogen oxides (NO_x), sulfur dioxide (SO_2), and hydrocarbons could lead to acid rain, depletion of the ozone (O_3) layer, and photochemical smog (Greaver et al., 2012). The average annual amounts of SO_2 and NO_x emitted by shipping have been reported to account for 5%–8% and 15% of the total emissions from anthropogenic sources, respectively (Eyring, 2005; Corbett et al., 2007). Shipping also emits high levels of particulate matter (PM) that includes organic carbon (OC), elemental carbon (EC), heavy metals, polycyclic aromatic hydrocarbons, sulfate, and nitrate, as well as secondary organic aerosols (SOAs) generated from gaseous precursors via atmospheric chemical processes (Sippula et al., 2014; Huang et al., 2018a). Owing to incomplete combustion, the carbonaceous aerosols (i.e., OC and EC) that dominate the PM emitted by shipping

* Corresponding author. Shanghai Institute of Eco-Chongming (SIEC), No. 3663 Northern Zhongshan Road, Shanghai, 200062, China.
** Corresponding author. Shanghai Key Laboratory of Atmospheric Particle Pollution and Prevention, Department of Environmental Science and Engineering, Institute of Atmospheric Sciences, Fudan University, Shanghai, 200433, China.
E-mail addresses: qli@fudan.edu.cn (Q. Li), jmchen@fudan.edu.cn (J. Chen).

https://doi.org/10.1016/j.jclepro.2019.117862
0959-6526/

(Wen et al., 2018) have negative impacts on global climate change, atmospheric visibility, and human health (Bond et al., 2013; McDonald et al., 2015). The particulate-bonded SO_4^{2-}, NO_3^-, and black carbon from shipping could contribute 2.3%–3.6%, 0.1%–2.3%, and 0.4%–1.4% of the global total emissions, respectively (Lauer et al., 2007). It has been reported that 12% of shipping-related PM has the potential to form cloud condensation nuclei (Hughes et al., 2000), which could affect atmospheric circulation and precipitation processes.

The contributions of pollutants emitted by ships and their negative impacts on atmospheric air quality are enhanced in the coastal regions of China (Fan et al., 2016; Liu et al., 2017), especially with regard to the ambient air quality of port cities. Among the top 10 busiest ports (in terms of cargo throughput) around the world, 7 are located in China (Chen et al., 2017). The throughput of container cargo volume reached 236.8 million twenty-feet equivalent (TEU) by the end of 2017 (MOT, 2017), 33% higher than that in 2012. With the high population density, people living in Chinese port cities are more vulnerable to greater health risks and more severe negative impacts from pollution than are their counterparts in foreign countries. It has been found that 20%–30% of $PM_{2.5}$ within 10 km of the coastline of Shanghai originate from ship emissions (Liu et al., 2017). Furthermore, SO_2, NO_x, and $PM_{2.5}$ emitted by ships are reportedly responsible for 12%, 9%, and 5.3% of total pollutant emissions in Shanghai, respectively (Fu et al., 2012). With the intention of mitigating shipping pollution, the Chinese government has established domestic emission control areas, including the Pearl River Delta, Yangtze River Delta, and Bohai Rim waters. The regulations limit the sulfur content of fuel oil to 0.5% (from 2019), while other pollutants such as NO_x, PM, and VOCs remain less strictly regulated. This outcome could be the result of insufficient field-based studies of ship emissions on which to base accurate regional-scale inventories.

Several real-world measurement campaigns have been recently conducted in China to investigate pollutant emissions. These have focused on the emission factors (EFs) of conventional gaseous (i.e., CO, NO_x, SO_2, and hydrocarbons) and particulate pollutants (PM_{10} and $PM_{2.5}$) (Zhang et al., 2016; Huang et al., 2018b), as well as on estimations of the total emission amounts of pollutants (Fan et al., 2016; Li et al., 2016a,b) and their relative contributions to ambient air pollution (Lv et al., 2018; Chen et al., 2019). Volatile organic compounds (VOCs) emitted by ships can produce O_3 in the atmosphere via complex chemical reactions with NO_x in the presence of sunlight (Hung-Lung et al., 2007). The generated O_3 can destroy ecosystems and reduce crop yields (Hassellöv et al., 2013). Moreover, VOCs can also be oxidized by hydroxyl and nitrate radicals to form low-volatile secondary organic compounds, which can enter the particulate phase as SOAs (Hoffmann et al., 1997). Thus, estimation of the VOC emissions from ships is of considerable importance for estimating their ozone formation potential (OFP) and SOA formation potential (SOAFP). This could provide fundamental data for further establishment of the characteristic spectrum of VOCs and achieve further control of pollutant emissions. However, systematic estimation of gaseous pollutants such as VOCs and key chemical components of PM in real-world ship emissions remains rare, especially for inland ports and vessels. Therefore, a systematic onboard study is urgently needed to improve the understanding of the atmospheric impact caused by pollutants in ship emissions.

In this study, the effects of engine speed and fuel type on the emission characteristics and atmospheric impacts of gaseous and particulate pollutants were estimated under several operating conditions. The fuel-based EFs of gaseous pollutants (including CO, SO_2, NO_x, and VOCs) and PM (including total suspended particles (TSP) and $PM_{2.5}$) were investigated, and the OFP and SOAFP of the quantified VOC species estimated. The obtained results are expected to improve the understanding of ship emissions and offer fundamental information to governments that support the implementation of well-defined emission standards.

2. Material and methods

2.1. Real-world emission measurements

The on-board ship emission campaign was conducted in June 2017. The measurements were obtained from two vessels: a container ship (AQ 7) and an inland cargo ship (HD 77). The length and breadth of HD 77 are 67 m and 12 m, respectively, and it is equipped with one main engine and two auxiliary engines. In this work, the emissions from the main engine of HD 77—a four-stroke four in-cylinder high-speed marine engine (Guizhou Tianli Diesel Engine Co., Ltd.)—were measured. This engine has a 135-mm bore, 150-mm stroke, rated engine speed of 1500 rpm, and rated power of 258.8 kW. In this investigation, the engine was operated with diesel oil (DO). AQ 7 is equipped with one main engine—a four-stroke six-cylinder in-line medium-speed marine diesel engine (GA6300ZCA, Ningbo Power and Machinery Group Co., Ltd.) operated using both heavy fuel oil (HFO) and DO—and four auxiliary engines. The properties, i.e., carbon content, viscosity at 40 °C, and flash point of HFO are 85.7%, 19.30 mm^2/s, and 66.0 °C, respectively, whereas those of DO are 80.02%, 2.93 mm^2/s, and 74.0 °C, respectively. Further details regarding the oils and the tests of AQ 7 with HFO and DO was presented in our previous study (Wu et al., 2018).

The routes followed by the two vessels during this study are shown in Fig. 1. AQ 7 departed from Qugang harbor (30.14°N, 122.09°E) in Zhejiang Province and arrived at Taicang (31.46°N, 121.13°E) in Jiangsu Province on June 19, 2017. The route of HD 77 was mainly within the coastal region of Chongming Island, which is located to the north of Shanghai. The ship started from the port of Daishan (30.24°N, 122.20°E) in Zhejiang Province, traveled across the East China Sea to the Yangtze River, and finally arrived at the port of Nantong (32.01°N, 120.81°E) in Jiangsu Province on June 27, 2017. Real-world emission tests were conducted under cruising modes. The ship features six engine speeds under 400, 450, 500, 550, 600, and 640 rpm, respectively. They were classified into low (400 and 450 rpm), medium (500 and 550 rpm), and high (600 and 640 rpm) engine speeds.

A schematic of the sampling system is displayed in Fig. S1. Detailed information can be found in our previous paper (Wu et al., 2018); hence, only a brief description is provided here. Gaseous pollutants, including CO, NO_x, SO_2, were determined using a flue gas analyzer (Testo 350, Germany), and VOC samples were collected using polyvinyl fluoride (PVF) bags. PM samples were collected on either quartz-fiber filters or Teflon filters for chemical analysis and determination of gravimetric weights. Size-segregated PM was sampled using a micro-orifice uniform deposit impactor. Three specimens were sampled concurrently for each test.

2.2. Chemical compositions of samples

A model 7100 pre-concentrator (Entech Inc., USA) was coupled with a 6890 gas chromatograph and 5973 mass spectrometer (Agilent, USA) to analyze 57 types of VOC species, including alkanes, alkenes, and aromatic hydrocarbons. All the collected PVF bags were analyzed within 24 h after collection. The details of the analysis method are provided in Zhang et al. (2012). A metals energy-dispersive X-ray fluorescence spectrometer (NAS100, Nayur Technology Co. Ltd., China) was employed to measure various selected elemental compositions. The elemental densities were examined directly after placing the filter on the sample stage with no pretreatment, as detailed in Li et al. (2016). Water-soluble ions

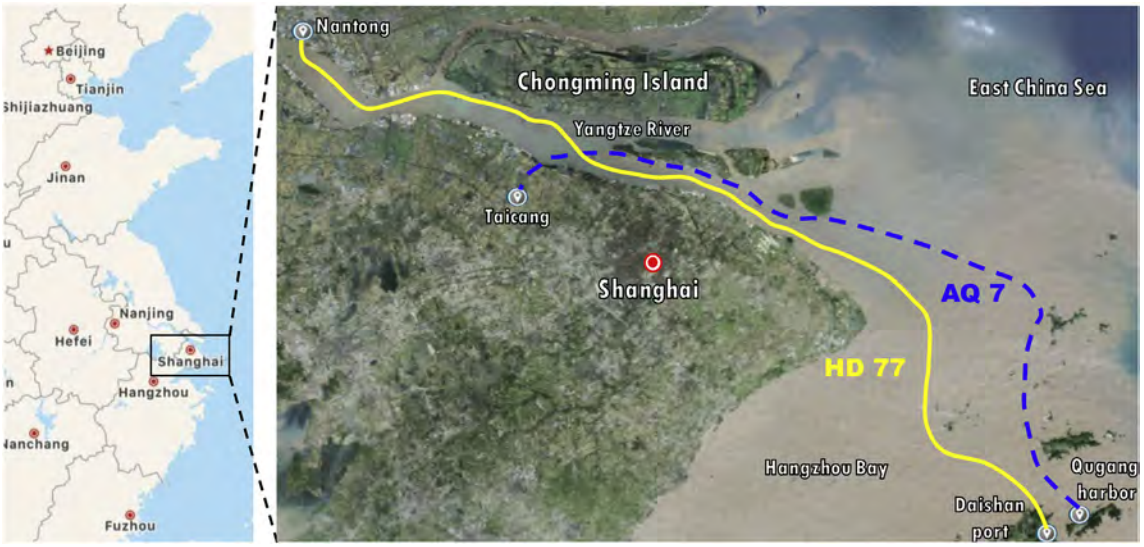

Fig. 1. Location of measurement site and routes of the container ship (AQ 7) and the inland vessel (HD 77). AQ 7 traveled from Qugang harbor (30.14°N, 122.09°E) in Zhejiang Province to Taicang (31.46°N, 121.13°E) in Jiangsu Province. HD 77 started from the port of Daishan (30.24°N, 122.20°E) in Zhejiang Province, passed Chongming Island via the Yangtze River waterway, and finally arrived at the port of Nantong (32.01°N, 120.81°E) in Jiangsu Province.

(WSIs) were examined using an ion chromatograph (940 Professional IC, Metrohm, Switzerland). A Metrosep A supp 16–250 column was applied for anions and a Metrosep C6 column was applied for cations. Recovery tests were conducted and recoveries of each ion were within 93%–102%. The carbonaceous composition (OC and EC) was analyzed following the Interagency Monitoring of Protected Visual Environments protocol. A 0.508 cm^2 sample of each specimen was punched and examined using a thermal/optical carbon analyzer (Model 2015, Atmoslytic Inc., Calabasas, CA, USA). Detailed descriptions of the sample analysis and quality control procedures are present in our previous paper (Wu et al., 2018).

2.3. Analysis method

Modified combustion efficiency (MCE) was determined using the following equation (Li et al., 2016a,b): $MCE = \Delta(CO_2)/(\Delta(CO_2) + \Delta(CO))$, where Δ signifies the molar concentration of the corresponding species. and OFP is estimated using the maximum incremental (MIR) coefficient method (Carter, 1994), which represents the maximum contribution of VOC species to the underground O_3 concentration under optimal conditions. The equation used for the estimation is as follows:

$$C_{j,OFP} = MIR_j \times C_{j,C} \times \frac{mj}{M}$$

where $C_{j,OFP}$ is the OFP of VOC species j, MIR_j represents the maximum incremental reaction coefficient for VOC species j, $C_{j,C}$ represents the observed concentration for VOC species j, m_j is the relative molecular mass of VOC species j, and M represents the relative molecular mass of O_3. The MIR values of the VOC components are listed in Table S1.

The SOAFP can be estimated using the following equation:

$$SOAFP = \sum_j EF_j \times Y_j$$

where EF_j represents the EF of species j, and Y_j is the SOA yield of species j. The SOA yields were estimated using two methods. The fractional aerosol coefficient (FAC) is commonly used in the estimation of reactive volatile organic species. The parameter is defined as the ratio of the SOA formation rate (kg/day) to the emission rate of the parent reactive organic gases. In this study, FAC values referenced from the works of Grosjean (Grosjean and Seinfeld, 1989; Grosjean, 1992) were adopted for alkanes. The yields for other species were adopted from Gentner et al. (2012), who calculated the yields of known species using chamber experiments combined with box modeling. All the referenced values are listed in Table S2.

3. Results and discussion

3.1. Effects of operating parameters on pollutant EFs

The parameters of the flue gases at the stack exit, including the MCE, flue gas temperature (T), and excess air ratio (λ) in different operating modes are shown in Fig. 2a. The temperature steadily increased with engine speed, varying in the range 227–403 °C at the stack exit. The trend in the variation of flue gas temperature suggests that the combustion temperature in the engine increases with engine speed (Rajkumar and Govindarajan, 2011). The excess air ratio, determining the fuel–air mixture, was in the range 1.85–2.99 and it showed a decreasing trend from lower to higher engine speed. The increase in exhaust gas temperature can be a function of increased load and reduced air excess ratio as the load (torque) of a ship engine typically increases with engine speed. The MCE, which ranged from 99.2% to 99.7%, first decreased and then increased with increasing engine speed. The MCE was found to correlate with both the combustion temperature and the excess air ratio (Flagan and Seinfeld, 2012), although their interrelationships are complex. Further studies should be conducted to investigate the relationships between the MCE, combustion temperature, and excess air ratio during the combustion process of DO in marine diesel engines.

The fuel-based EFs of pollutants at different engine speeds are displayed in Fig. 2b. The EFs of CO ranged from 11.7 ± 0.5 to 30.1 ± 2.4 g/kg fuel. Sulfur can be oxidized by oxygen to form SO_2 during the combustion process. The EFs of SO_2 tended to decrease toward higher engine speeds, which is attributable mainly to the lower oxygen concentration found at high engine speeds. Several

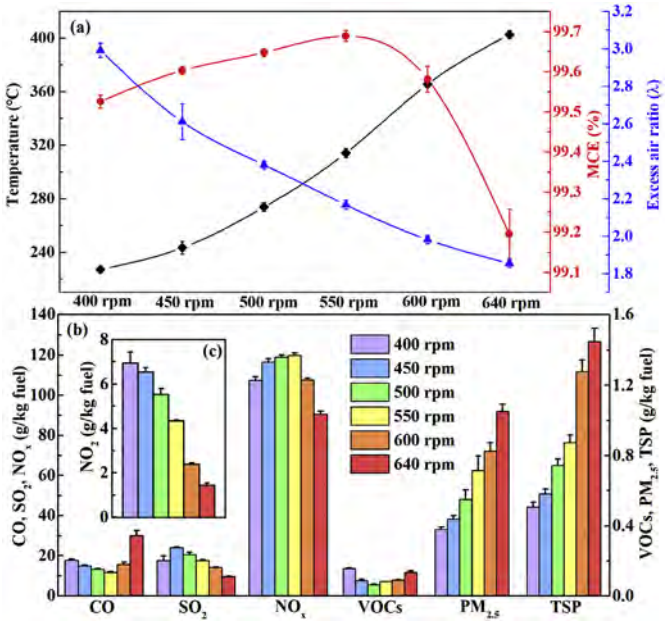

Fig. 2. (a) Combustion parameters under different engine speeds, including modified combustion efficiency (MCE), temperature (T), and excess air ratio (λ). (b) Fuel-based emission factors (EFs) for gaseous and particulate pollutants at different engine speeds, including CO, SO_2, NO_x, VOCs, $PM_{2.5}$, and TSP. (c) Fuel-based emission factors for NO_2. EFs of NO_x under different operational modes correlated positively with the MCE ($r = 0.96$, $p = 0.002$).

factors can influence NO_x formation in marine diesel engines, including the excess air ratio, temperature, pressure, and time of fuel injection. The main constituent of NO_x is NO, comprising 94%–98% of the total NO_x. As most NO is formed via the thermal NO mechanism during the combustion process (Haglind, 2008), sufficient oxygen concentration and high temperature are prerequisites for NO formation. The EFs of NO_x for different operating modes were found to be positively correlated with the MCE ($r = 0.96$, $p = 0.002$), which contributed 96% of the variation to the EFs of NO_x. The maximum value of the EFs of NO_x was observed at 550 rpm. This could be related to the high oxygen concentration ($\lambda = 2.17$) and high temperature ($T = 314\,^{\circ}C$) under such operational conditions, which resulted in a high rate of NO formation. The minimum value of the EFs of NO_x was found at the highest engine speed, which could be attributable to the low oxygen concentration ($\lambda = 1.85$). NOx emissions are also correlated with combustion timing, which may differ with engine speed and load. The EFs of NO_2 exhibited a decreasing trend with increasing engine speed, displaying a tendency similar to λ. As the oxygen concentration in the combustion chamber plays a vital role in the formation of NO_2 (Rößler et al., 2017), higher oxygen content can promote greater NO_2 formation, as shown in Fig. 2c. The EFs of the VOCs first decreased and then increased with increasing engine speed, exhibiting a trend opposite to that of the MCE. This reverse trend suggests that incomplete combustion is the principal reason for high VOC emissions in diesel engines.

The EFs of the TSP ranged from 0.51 ± 0.03 to 1.45 ± 0.07 g/kg fuel, and the EFs of $PM_{2.5}$ varied between 0.38 ± 0.01 and 1.05 ± 0.05 g/kg fuel, exhibiting an increasing trend toward higher engine speeds. The PM in the exhaust of diesel engines comprises a complex mixture of soot, ash, the condensable organic fraction, metals, and sulfates absorbed onto soot particles. The formation of PM is a complex process that includes thermal cracking and pyrolysis, dehydrogenation, agglomeration, adsorption, and condensation (Kittelson et al., 2006). The EFs of PM under different operating modes were found to correlate positively with flue temperature ($p = 0.002$) and negatively with the excess air ratio ($p = 0.01$). The flue temperature and the excess air ratio contributed 97% and 89% of the variation to the EFs of PM, respectively. High temperature and oxygen deficiency could lead to greater formation of soot (Li et al., 2014), which would translate to higher soot concentration at higher engine speeds. This tendency is further illustrated in Fig. 3.

The EFs of pollutants for AQ 7 when operated with HFO and DO are shown in Fig. S2. It is clear that fuel type has a considerable effect on the EFs of pollutants, including SO_2, VOCs, $PM_{2.5}$, and TSP. The EFs of the pollutants emitted by the ship during combustion of HFO were found to be much higher than during the combustion of DO, primarily because of the incomplete combustion process when operating the engine with HFO.

3.2. Effect of engine speed on particulate composition

The $PM_{2.5}$ EFs and their chemical compositions as a function of engine speed are shown in Fig. 3. Organic matter is estimated via OC × 1.2 (Petzold et al., 2008). Carbonaceous particles, including OC and EC, are the major components of $PM_{2.5}$, which accounted for 67.9%–73.9% of the total $PM_{2.5}$ mass concentration. The OC/EC ratio varied between 0.31 and 1.81, which is much lower than that from large cargo vessels (Moldanová et al., 2009; Huang et al., 2018b). The difference in OC and EC emissions could be attributed to engine type (Lack et al., 2009). The mass fractions of EC/$PM_{2.5}$ were 24%–56% and generally higher at higher engine speeds. It indicates that a higher fraction of EC is contained within the exhaust of a ship at higher engine speeds. Higher engine speeds induce higher temperature and lower oxygen concentration, which promote soot formation (Li et al., 2014). Highly reactive NO_2 could promote soot oxidation, and the NO_2/NO_x ratio was applied to reflect the oxidizing ability of the flue gas (Rößler et al., 2017), which tended to decrease with increasing engine speed. The results exhibited a trend similar to the EFs of SO_2 because insufficient oxygen cannot adequately promote sulfur oxidation. Soot oxidation could be inhibited owing to lack of reactive oxygen species, leading to higher $PM_{2.5}$ emissions and higher TSPs at higher engine speeds. The oxidizing ability was found to correlate significantly with the EC/$PM_{2.5}$ ratio. The linear fit of oxidizing ability has a relationship of

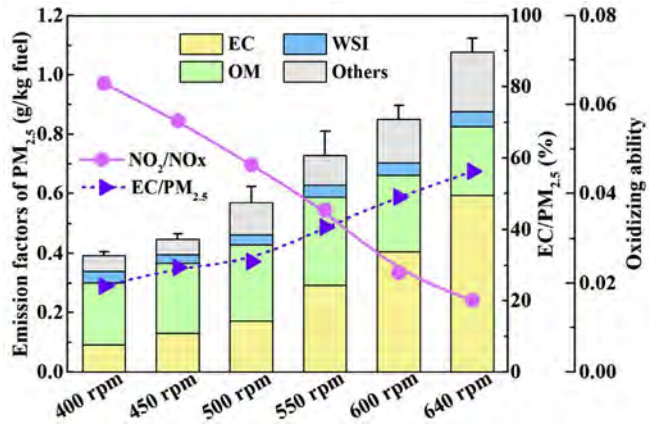

Fig. 3. EFs and chemical compositions of $PM_{2.5}$, including organic matter (OM) (OM = OC × 1.2), EC, metals, WSI, and others, which comprised metals and other negligible mass fraction species. The pink line indicates the defined oxidizing ability (1.6%–6.5%) and the dashed purple line indicates the mass ratio of EC in $PM_{2.5}$ (24%–56%). The oxidizing ability was found to correlate significantly with the EC/$PM_{2.5}$ ratio ($r = -0.98$, $p < 0.001$). (For interpretation of the references to colour in this figure legend, the reader is referred to the Web version of this article.)

$y = -0.15x + 9.85$, where y and x represent the volume ratio of NO_2/NO_x and the mass ratio of $EC/PM_{2.5}$, respectively. The correlation coefficient (r) is −0.98 and the p value is < 0.001, as shown in Fig. S3.

The EFs of the WSIs varied between 29.5 and 49.5 mg/kg fuel, which contributed 4.7%–10.0% to the total $PM_{2.5}$ mass concentration. The mass fraction of the WSIs in the $PM_{2.5}$ samples decreased with engine speed, as shown in Fig. S4. The decreasing tendency of WSIs is consistent with the increasing tendency of $EC/PM_{2.5}$. Sulfate was the dominant ion in the PM, followed by NH_4^+, Ca^{2+}, NO_3^-, Na^+, and Cl^-. The fractions of sulfate in the $PM_{2.5}$ varied in the range 2.9%–6.1%, while the NH_4^+ fractions were found to be between 1.2% and 2.6%. Some organic acids such as formic acid (HCOOH) and oxalic acid ($H_2C_2O_4$) could be examined in the PM samples. The EFs of HCOOH and $H_2C_2O_4$ were found to be in the ranges 0.08–0.29 and 0.20–0.65 mg/kg fuel, respectively. This indicates that ship emissions constitute important anthropogenic sources of low molecular organic acid emissions, which play an important role in the production of oxygenated VOCs (Takegawa et al., 2007). Metal species were found in low concentrations in the PM emissions, contributing 0.4%–1.3% to the total $PM_{2.5}$ mass concentration. The dominant elements in the PM were Ca and Fe, followed in descending order by Si, Mg, and Zn. The results were found to be consistent with a previous study (Huang et al., 2018b). The metal composition was found to vary with fuel type; V dominated the emissions from HFO (Wu et al., 2018), but was not present in the emissions of DO.

3.3. Emission profiles of VOC species

Fifty-seven VOC species were quantified in the gaseous samples. The EFs of the VOC species, also primarily the result of incomplete combustion, are presented as a function of ship operation at different engine speeds in Fig. 4a. The EFs of the VOCs first decreased and then tended to increase with increasing engine speed, exhibiting a tendency opposite to that of the MCE. This could be because lower combustion efficiency is the main reason for higher VOC emissions. Aromatics and alkenes were the main components of the quantified VOC species, contributing 26%–74% and 12%–63% to the total VOCs, respectively, while alkanes and acetylene were relatively low, comprising 11%–23% and 1%–13% of the total VOCs, respectively (see Fig. 4b). The highest value of aromatic EFs was found at 640 rpm. This is because high temperature and a low air–fuel ratio are optimal conditions for the formation of aromatics. The EFs of acetylene presented a trend opposite to that of the aromatics, indicating that the formation of aromatics might be primarily via the hydrogen-abstraction-C_2H_2-addition mechanism (Tree and Svensson, 2007). The proportion of individual VOC species varied significantly with engine speed. It was found that 1,2,4-trimethylbenzene, m-ethyl toluene, and benzene were the main species in the VOC samples when the engine was operated at high speed, comprising 16.7%, 12.5%, and 6.8% of the total VOCs. Ethylene was found to be the most abundant VOC in the ship exhaust under low and medium engine speeds, accounting for 12.0%–36.1% of the total VOCs.

Fuel type had a significant influence on the emissions of VOC species and concentrations, as illustrated in Fig. 5. The EFs of the VOCs of HFO were 3.3 times higher than those of DO. Ethylene was found to be the dominant species, responsible for approximately 45% and 39% of the total VOCs in the HFO and DO samples, respectively. The major species in the HFO VOCs were propene, acetylene, and benzene, which contributed 11.2%, 9.8%, and 8.6% to the total VOCs, respectively. However, the major species in the DO VOCs were acetylene, benzene, and m-ethyl toluene, accounting for 9.4%, 5.6%, and 5.4% of the total VOCs, respectively. The EFs of aromatics and their mass fractions are shown in Fig. S5. The distributions of aromatics were reasonably similar at various engine speeds. The four species—i.e., 1,2,4-trimethylbenzene, benzene,

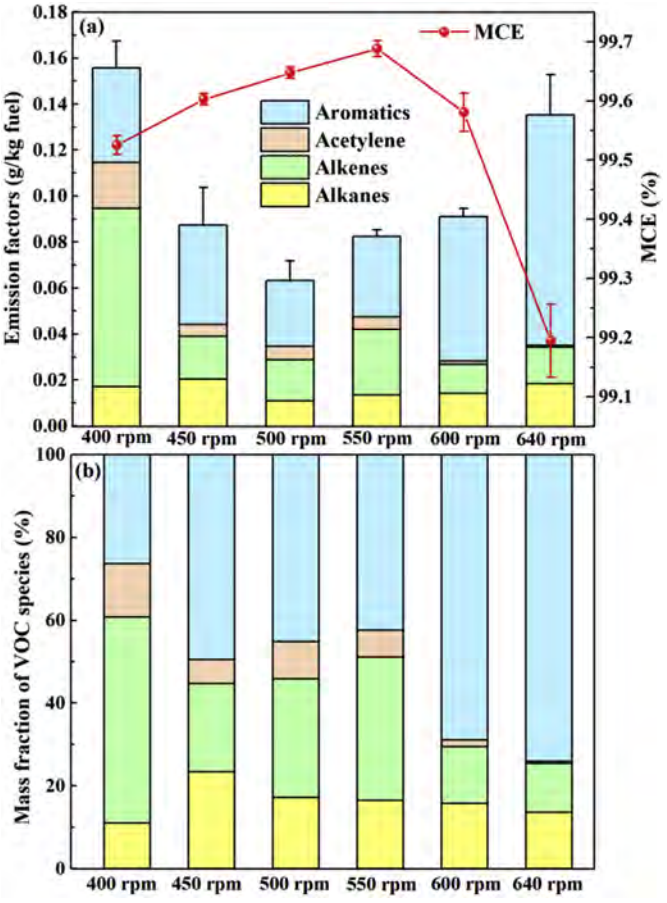

Fig. 4. (a) Emission characteristics of VOC species based on engine speed. Red line indicates the MCE. (b) Mass fraction of VOC species. VOCs species are classified into alkanes, alkenes, acetylene, and aromatics. (For interpretation of the references to colour in this figure legend, the reader is referred to the Web version of this article.)

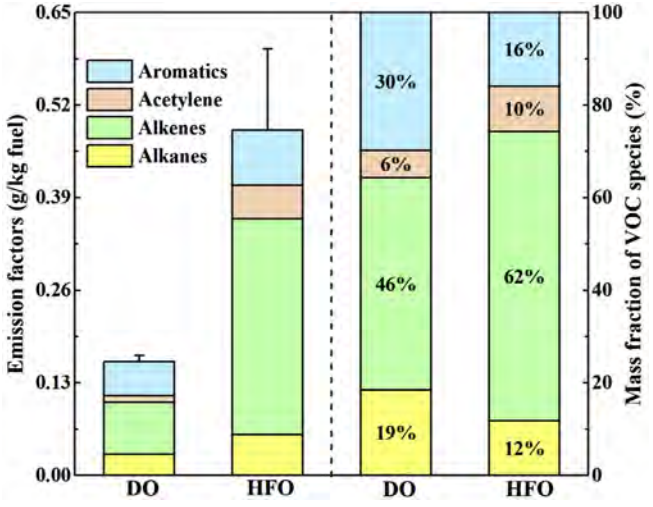

Fig. 5. Emission characteristic of VOC species from a four-stroke six-cylinder in-line medium-speed marine diesel engine (GA6300ZCA, build: Ningbo Power and Machinery Group Co., Ltd.) based on fuel type, including alkanes, alkenes, acetylene, and aromatics. The engine speed was approximately 380 rpm or 400 rpm in cruising mode.

toluene, and m-ethyl toluene—together comprised 57%–65% of the total aromatics. Benzene dominated the aromatics in the HFO sample, followed by toluene—accounting for 54% and 21% of the total aromatic emissions, respectively. For the DO sample, benzene was the most abundant aromatic species, followed by m-ethyl toluene, 1,2,4-trimethylbenzene, and toluene—accounting for 20%, 17%, 15%, and 13% of the total aromatics, respectively. The VOCs emitted from different engines were reasonably similar when operated with DO at the same engine speed.

3.4. OFP and SOAFP of VOCs in ship emissions

Engine speed has a significant influence on the OFP of the VOCs in ship emissions. The results unified into g O_3/kg fuel are shown in Fig. 6a. The OFP varied between 0.33 and 0.83 g O_3/kg fuel. It was found that the VOCs in the ship exhausts generated more O_3 at high or low engine speeds than at medium engine speed primarily because of the higher VOC emissions caused by lower combustion efficiency. The contributions of the examined VOC species to the OFP are presented in Fig. 6b. Aromatics and alkenes had the greatest influence on the OFP, accounting for 24%–83% and 15%–73% of O_3 formation, respectively. Most alkenes and aromatics have a high MIR coefficient (Carter, 1994), which could contribute a larger fraction to the OFP. Ethylene, propene, and 1,2,4-trimethylbenzene were the primary species that contributed to O_3 formation under low or medium engine speeds, together accounting for 48.7%–73.6% of the OFP values. At high engine speeds, 1,2,4-trimethylbenzene, m-ethyl toluene, and 1,3,5-trimethylbenzene were the main contributors to the formation of O_3, comprising approximately 49% of the OFP. However, the SOAFP showed a different tendency to the OFP, as illustrated in Fig. 6c. The SOA generation varied in the range 2.8–8.9 mg SOA/kg fuel. Aromatics contributed substantially to the SOAFP, accounting for 90%–98% of the total SOAFP. Benzene, 1,2,4-trimethylbenzene, and toluene were the main contributors to SOA formation under low or medium engine speeds, together comprising 52.5%–58.1% of the SOAFP. At high engine speeds, 1,2,4-trimethylbenzene, m-ethyl toluene, and benzene were the main contributors to SOA formation, contributing ~52.2% of the SOAFP, primarily because of their large emissions and high SOA yields. The mass size distribution of TC dominated in the accumulation mode, which adsorbed volatile precursors to form SOA via gas-to-particle conversion, as shown in Fig. S6 (Kittelson et al., 2006). As intermediate VOCs (IVOCs), which have higher SOA yields, were not identified in this study, the SOAFP could be underestimated in this work (Zhao et al., 2014). The OFP values unified into g O_3/g VOCs are displayed in Fig. S7a; they exhibit reasonably similar trends at all engine speeds. The SOAFP results unified into g SOA/g VOCs are displayed in Fig. S7b.

The effects of fuel type on the OFP and the SOAFP are shown in Fig. 7. The amounts of O_3 and SOAs generated by burning HFO were found to be ~3.3- and ~2.1-fold higher, respectively, than from burning DO. Alkenes dominated the OFP in the HFO sample, accounting for 90% of the total OFP. However, for the DO sample, alkenes and aromatics were the major contributors, accounting for 64% and 32% of the total OFP, respectively. In term of individual species, ethylene made the largest contribution to the OFP for HFO, followed by propene, contributing 62.4% and 19.8% of the total OFP, respectively. For DO, ethylene was the species with the largest OFP followed by 1,2,4-trimethylbenzene and m-ethyl toluene, comprising 59.7%, 8.1%, and 7.9% of the total OFP, respectively. Aromatics were the main contributor to the SOAFP for both HFO and DO samples, accounting for 94% and 96%, respectively. The top three main species for the SOAFP in the HFO sample were benzene, toluene, and 1,2,4-trimethylbenzene, contributing 66.0%, 15.1%, and 2.7% of the total SOAFP, respectively. M-ethyl toluene dominated the SOAFP in the DO sample followed by toluene and 1,2,4-trimethylbenzene, accounting for 17.9%, 8.2%, and 7.9% of the total SOAFP, respectively. Based on the emission profiles of VOC species,

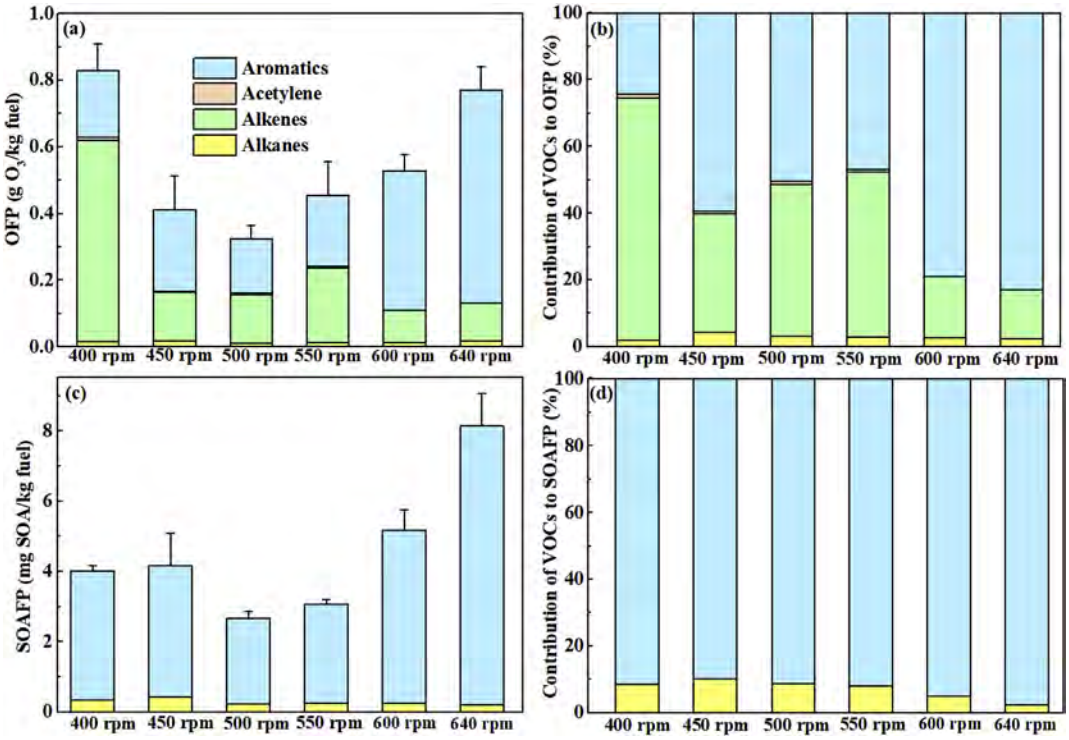

Fig. 6. (a) OFP (in g O_3/kg fuel) from VOC species (including alkanes, alkenes, acetylene, and aromatics) based on engine speed, (b) contribution of VOC species to OFP, (c) SOAFP (in mg SOA/kg fuel) from VOC species (including alkanes and aromatics) based on engine speed, and (d) contribution of VOC species to SOAFP.

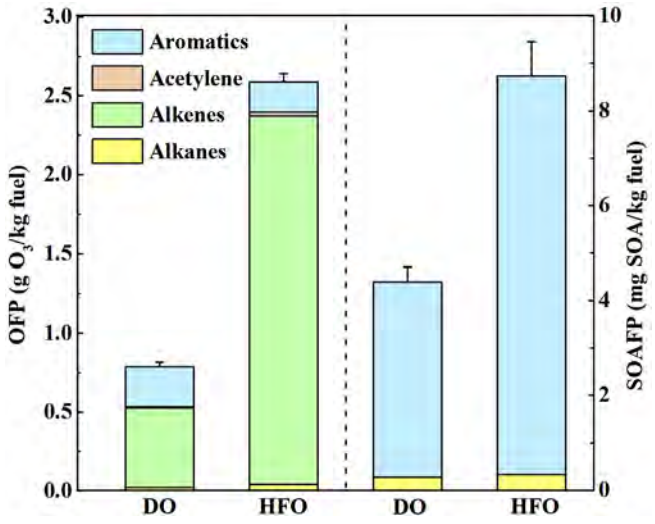

Fig. 7. OFP (in g O_3/kg fuel) from VOC species (including alkanes, alkenes, acetylene, and aromatics) and SOAFP (in mg SOA/kg fuel) from VOC species (including alkanes and aromatics) in a four-stroke six-cylinder in-line medium-speed marine diesel engine (GA6300ZCA, build: Ningbo Power and Machinery Group Co., Ltd.) based on fuel type. The engine speed was approximately 380 rpm or 400 rpm in cruising mode.

ship emissions could be a significant source for ground-level O_3 and SOAs in coastal areas. The OFP and SOAFP results unified into g O_3/g VOCs and g SOA/g VOCs are displayed in Fig. S8.

3.5. Environmental implications

Pollutants emitted in the ship exhaust were found to vary considerably under different operating conditions. Operation at medium engine speeds produced much lower values of VOC EFs, OFP, and SOAFP but higher values of NO_x EFs than at low and high engine speeds, mainly owing to the higher combustion efficiency. The average reductions in the values of VOC EFs, OFP, and SOAFP were 35.0%, 29.2%, and 29.8%, respectively, in comparison with the low engine speed, respectively, while those were 33.2%, 37.8%, and 54.7% compared to the high engine speed, respectively. For PM EFs, operating at a medium engine speed led to a reduction of 32% compared to high engine speed, whereas it increased by 55% compared with low engine speed. Use of DO, which is a high-quality fuel, could alleviate pollutant emissions, as shown in Fig. S2. The reductions in the EFs of SO_2, VOCs, $PM_{2.5}$, and TSP were 50%, 67%, 42%, and 66%, respectively. The lower EFs of VOCs when switching from HFO to DO mean that the OFP and the SOAFP can be reduced by 70% and 52%, respectively. However, NO_x EFs were found higher during DO combustion relative to HFO combustion. These results suggest that further real-world measurements and estimations should be conducted to determine the optimal engine speed based on pollutant EFs. In addition, emission abatement technologies such as selective catalytic reduction or exhaust gas recirculation should be applied to marine diesel engines to realize NO_x emission limits. The average VOC emissions, calculated as the product of shipping fuel consumption and VOC EFs, were estimated at approximately 8.96 Gg in Shanghai, which could constitute ~22% of the total VOCs found in the exhaust of on-road vehicles, as reported in Wu and Xie (2017). The results indicate that ship emissions constitute an important anthropogenic source of VOC species in coastal regions. Hence, relevant regulations and emission standards regarding VOCs in the exhaust of ships should be implemented to alleviate air pollution.

The OFP and SOAFP of VOC species exhausted from various mobile sources are compared in Table 1. Each value has been normalized to units of g VOC. The results indicate that the VOCs emitted from container ships have greater potential to generate O_3 and SOAs than those from on-road vehicle emissions (Tsai et al., 2012; Huang et al., 2015; Yao et al., 2015). The average OFP and SOAFP of ship emissions are ~2.3- and ~2.6-fold greater than from diesel vehicles. The VOC species in the exhaust of ships could be a major contributor to O_3 and SOA formation in port cities. As the OFP and SOAFP of container ships were found to be higher than for many mobile sources, the environmental impact of such ships cannot be overlooked, particularly in coastal regions (Contini et al., 2011). The values derived in this study for a container ship are slightly higher than those reported by Xiao et al. (2018). This difference may be a reflection of the various types of VOC species emitted by ships when operating with different fuel types and different engines.

4. Conclusions

The effects of engine speed and fuel type on the pollutants exhausted by ships were investigated in this study. The pollutant emissions varied considerably depending on engine speed, with the EFs of CO exhibiting high values at low or high engine speeds. The highest NO_x EF was observed at medium engine speed. The VOC EFs were lowest at medium engine speed, which resulted in lower OFP and SOAFP values. The EFs of PM tended to increase with increasing engine speed. Fuel quality was also found to influence pollutant emissions considerably. The use of high-quality fuel is of great importance for reducing the emission of pollutants, except NO_x. Switching from HFO to DO decreased the EFs of SO_2, VOCs, $PM_{2.5}$, and TSP by 50%, 67%, 42%, and 66%, respectively. Using DO reduced ground-level O_3 and SOA emissions because of the lower EFs of VOC species. Estimation of the environmental impact demonstrated that the VOCs emitted by container ships generate higher levels of O_3 and SOAs than those from on-road vehicles, which can have an adverse effect on air quality and ecosystems, particularly in coastal regions. These results suggest that emission abatement technologies such as selective catalytic reduction or exhaust gas recirculation should be applied to marine diesel engines to mitigate pollutant emissions. Furthermore, stringent

Table 1
Comparison between the OFP and the SOAFP of VOC species of ship and on-road vehicle emissions in this and previous studies.

Emission source	OFP (g O_3/g VOCs)	SOAFP (g SOA/g VOCs)	Fuel Type	Reference
Light-duty diesel vehicles	2.31 ± 1.20	0.015 ± 0.006	diesel	Tsai et al.,2012
Light-duty diesel trucks	1.93 ± 0.23	0.007 ± 0.001	diesel	Yao et al. (2015)
Heavy-duty diesel trucks	2.44 ± 0.23	0.013 ± 0.002	diesel	Huang et al. (2015)
Container ship	2.63 ± 0.37	0.017 ± 0.007	MDO	Xiao et al. (2018)
Container ship	5.34 ± 0.18	0.018 ± 0.005	HFO (AQ 7)	This study
	4.92 ± 0.27	0.027 ± 0.002	DO (AQ 7)	
	5.32 ± 0.41	0.045 ± 0.013	DO (HD 77)	

MDO: Marine diesel oil; HFO: Heavy fuel oil; DO: diesel oil.

regulations should be imposed on pollutant emissions from ships to improve regional air quality. Further, VOC species, particularly aromatics, should be controlled preferentially because of their substantial contributions to regional O_3 and particulate pollution.

Declaration of interest

None.

Acknowledgments

This work was supported by the Ministry of Science and Technology of China (grant numbers 2016YFC0202700, 2018YFC0213800); the National Natural Science Foundation of China (grant numbers 91743202, 41805091); and the Natural Science Foundation of Shanghai (grant number 18ZR1403000).

Appendix A. Supplementary data

Supplementary data to this article can be found online at https://doi.org/10.1016/j.jclepro.2019.117862.

References

Bond, T.C., Doherty, S.J., Fahey, D.W., Forster, P.M., Berntsen, T., DeAngelo, B.J., Flanner, M.G., Ghan, S., Karcher, B., Koch, D., Kinne, S., Kondo, Y., Quinn, P.K., Sarofim, M.C., Schultz, M.G., Schulz, M., Venkataraman, C., Zhang, H., Zhang, S., Bellouin, N., Guttikunda, S.K., Hopke, P.K., Jacobson, M.Z., Kaiser, J.W., Klimont, Z., Lohmann, U., Schwarz, J.P., Shindell, D., Storelvmo, T., Warren, S.G., Zender, C.S., 2013. Bounding the role of black carbon in the climate system: a scientific assessment. J. Geophys. Res. 118 (11), 5380–5552.

Carter, W.P.L., 1994. Development of ozone reactivity scales for volatile organic compounds. Air Waste 44 (7), 881–899.

Chen, D., Tian, X., Lang, J., Zhou, Y., Li, Y., Guo, X., Wang, W., Liu, B., 2019. The impact of ship emissions on PM2.5 and the deposition of nitrogen and sulfur in Yangtze River Delta, China. Sci. Total Environ. 649, 1609–1619.

Chen, D., Wang, X., Nelson, P., Li, Y., Zhao, N., Zhao, Y., Lang, J., Zhou, Y., Guo, X., 2017. Ship emission inventory and its impact on the PM 2.5 air pollution in Qingdao Port, North China. Atmos. Environ. 166, 351–361.

Contini, D., Gambaro, A., Belosi, F., De Pieri, S., Cairns, W.R.L., Donateo, A., Zanotto, E., Citron, M., 2011. The direct influence of ship traffic on atmospheric PM2.5, PM10 and PAH in Venice. J. Environ. Manag. 92 (9), 2119–2129.

Corbett, J.J., Winebrake, J.J., Green, E.H., Kasibhatla, P., Eyring, V., Lauer, A., 2007. Mortality from ship emissions: a global assessment. Environ. Sci. Technol. 41 (24), 8512.

Eyring, V., 2005. Emissions from international shipping: 1. The last 50 years. J. Geophys. Res. 110 (D17305), 17305–17317.

Eyring, V., Isaksen, I.S.A., Berntsen, T., Collins, W.J., Corbett, J.J., Endresen, O., Grainger, R.G., Moldanova, J., Schlager, H., Stevenson, D.S., 2010. Transport impacts on atmosphere and climate: Shipping. Atmos. Environ. 44 (37), 4735–4771.

Fan, Q., Zhang, Y., Ma, W., Ma, H., Feng, J., Yu, Q., Yang, X., Ng, S.K., Fu, Q., Chen, L., 2016. Spatial and seasonal dynamics of ship emissions over the Yangtze River Delta and East China Sea and their potential environmental influence. Environ. Sci. Technol. 50 (3), 1322–1329.

Flagan, R.C., Seinfeld, J.H., 2012. Fundamentals of Air Pollution Engineering. Courier Dover Publications, New Jersey.

Fu, Q.Y., Shen, Y., Zhang, J., 2012. On the ship pollutant emission inventory in Shanghai port (in Chinese). J. Saf. Environ. 12 (5), 57–64.

Gentner, D.R., Isaacman, G., Worton, D.R., Chan, A.W.H., Dallmann, T.R., Davis, L., Liu, S., Day, D.A., Russell, L.M., Wilson, K.R., Weber, R., Guha, A., Harley, R.A., Goldstein, A.H., 2012. Elucidating secondary organic aerosol from diesel and gasoline vehicles through detailed characterization of organic carbon emissions. Proc. Natl. Acad. Sci. U. S. A 109 (45), 18318–18323.

Greaver, T., Sullivan, T., Herrick, J., C Barber, M., Baron, J., Cosby, B., E Deerhake, M., L Dennis, R., B Dubois, J.-J., L Goodale, C., Herlihy, A., Lawrence, G., Liu, L., Lynch, J., J Novak, K., 2012. Ecological effects of nitrogen and sulfur air pollution in the US: what do we know? Front. Ecol. Environ. 10 (8), 365–372.

Grosjean, D., 1992. Insitu organic aerosol formation during a smog episode - estimated production and chemical functionality. Atmos. Environ. 26 (6), 953–963.

Grosjean, D., Seinfeld, J.H., 1989. Parameterization of the formation potential of secondary organic aerosols. Atmos. Environ. 23 (8), 1733–1747.

Haglind, F., 2008. A review on the use of gas and steam turbine combined cycles as prime movers for large ships. Part I: background and design. Energy Convers. Manag. 49 (12), 3458–3467.

Hassellöv, I.-M., Turner, D.R., Lauer, A., Corbett, J., 2013. Shipping contributes to ocean acidification. Geophys. Res. Lett. 40, 2731–2736.

Hoffmann, T., Odum, J.R., Bowman, F., Collins, D., Klockow, D., Flagan, R.C., Seinfeld, J.H., 1997. formation of organic aerosols from the oxidation of biogenic hydrocarbons. J. Atmos. Chem. 26 (2), 189–222.

Huang, C., Hu, Q.Y., Li, Y.J., Tian, J.J., Ma, Y.G., Zhao, Y.L., Feng, J.L., An, J.Y., Qiao, L.P., Wang, H.L., Jing, S.A., Huang, D.D., Lou, S.R., Zhou, M., Zhu, S.H., Tao, S.K., Li, L., 2018. Intermediate volatility organic compound emissions from a large cargo vessel operated under real-world conditions. Environ. Sci. Technol. 52 (21), 12934–12942.

Huang, C., Hu, Q.Y., Wang, H.Y., Qiao, L.P., Jing, S.A., Wang, H.L., Zhou, M., Zhu, S.H., Ma, Y.G., Lou, S.R., Li, L., Tao, S.K., Li, Y.J., Lou, D.M., 2018. Emission factors of particulate and gaseous compounds from a large cargo vessel operated under real-world conditions. Environ. Pollut. 242, 667–674.

Huang, C., Wang, H.L., Li, L., Wang, Q., Lu, Q., de Gouw, J.A., Zhou, M., Jing, S.A., Lu, J., Chen, C.H., 2015. VOC species and emission inventory from vehicles and their SOA formation potentials estimation in Shanghai, China. Atmos. Chem. Phys. 15 (19), 11081–11096.

Hughes, L.S., Allen, J.O., Bhave, P., Kleeman, M.J., Cass, G.R., Liu, D.Y., Fergenson, D.F., Morrical, B.D., Prather, K.A., 2000. Evolution of atmospheric particles along trajectories crossing the Los Angeles basin. Environ. Sci. Technol. 34 (15), 3058–3068.

Hung-Lung, C., Jiun-Horng, T., Shih-Yu, C., Kuo-Hsiung, L., Sen-Yi, M., 2007. VOC concentration profiles in an ozone non-attainment area: a case study in an urban and industrial complex metroplex in southern Taiwan. Atmos. Environ. 41 (9), 1848–1860.

Kittelson, D.B., Watts, W.F., Johnson, J.P., 2006. On-road and laboratory evaluation of combustion aerosols - Part 1: summary of diesel engine results. J. Aerosol Sci. 37 (8), 913–930.

Lack, D.A., Corbett, J.J., Onasch, T., Lerner, B., Massoli, P., Quinn, P.K., Bates, T.S., Covert, D.S., Coffman, D., Sierau, B., Herndon, S., Allan, J., Baynard, T., Lovejoy, E., Ravishankara, A.R., Williams, E., 2009. Particulate emissions from commercial shipping: chemical, physical, and optical properties. J. Geophys. Res. 114, D00F04–D00F19.

Lauer, A., Eyring, V., Hendricks, J., Jöckel, P., Lohmann, U., 2007. Global model simulations of the impact of ocean-going ships on aerosols, clouds, and the radiation budget. Atmos. Chem. Phys. 7 (19), 5061–5079.

Li, C., Yuan, Z., Ou, J., Fan, X., Ye, S., Xiao, T., Shi, Y., Huang, Z., Ng, S.K., Zhong, Z., Zheng, J., 2016. An AIS-based high-resolution ship emission inventory and its uncertainty in Pearl River Delta region, China. Sci. Total Environ. 573, 1–10.

Li, Q., Jiang, J., Cai, S., Zhou, W., Wang, S., Duan, L., Hao, J., 2016. Gaseous ammonia emissions from coal and biomass combustion in household stoves with different combustion efficiencies. Environ. Sci. Technol. Lett. 3 (3), 98–103.

Li, X., Xu, Z., Guan, C., Huang, Z., 2014. Particle size distributions and OC, EC emissions from a diesel engine with the application of in-cylinder emission control strategies. Fuel 121, 20–26.

Lin, H., Tao, J., Qian, Z.M., Ruan, Z., Xu, Y., Hang, J., Xu, X., Liu, T., Guo, Y., Zeng, W., Xiao, J., Guo, L., Li, X., Ma, W., 2018. Shipping pollution emission associated with increased cardiovascular mortality: a time series study in Guangzhou, China. Environ. Pollut. 241, 862–868.

Liu, Z., Lu, X., Feng, J., Fan, Q., Zhang, Y., Yang, X., 2017. Influence of ship emissions on urban air quality: a comprehensive study using highly time-resolved online measurements and numerical simulation in Shanghai. Environ. Sci. Technol. 51 (1), 202–211.

Lv, Z., Liu, H., Ying, Q., Fu, M., Meng, Z., Wang, Y., Wei, W., Gong, H., He, K., 2018. Impacts of shipping emissions on PM2.5 pollution in China. Atmos. Chem. Phys. 18 (21), 15811–15824.

McDonald, B.C., Goldstein, A.H., Harley, R.A., 2015. Long-term trends in California mobile source emissions and ambient concentrations of black carbon and organic aerosol. Environ. Sci. Technol. 49 (8), 5178–5188.

Moldanová, J., Fridell, E., Popovicheva, O., Demirdjian, B., Tishkova, V., Faccinetto, A., Focsa, C., 2009. Characterisation of particulate matter and gaseous emissions from a large ship diesel engine. Atmos. Environ. 43 (16), 2632–2641.

MOT, 2017. The Statistical Report on China's Traffic in 2017 (In Chinese). China Statistics Press, Beijing.

Petzold, A., Hasselbach, J., Lauer, P., Baumann, R., Franke, K., Gurk, C., Schlager, H., Weingartner, E., 2008. Experimental studies on particle emissions from cruising ship their characteristic properties transformation and atmospheric lifetime in the marine boundary layer. Atmos. Chem. Phys. 8, 2387–2403.

Rößler, M., Koch, T., Janzer, C., Olzmann, M., 2017. Mechanisms of the NO2 formation in diesel engines. MTZ worldwide 78 (7), 70–75.

Rajkumar, K., Govindarajan, P., 2011. Impact of oxygen enriched combustion on the performance of a single cylinder diesel engine. P. Front. Energy. 5 (4), 398–403.

Sippula, O., Stengel, B., Sklorz, M., Streibel, T., Rabe, R., Orasche, J., Lintelmann, J., Michalke, B., Abbaszade, G., Radischat, C., Groger, T., Schnelle-Kreis, J., Harndorf, H., Zimmermann, R., 2014. Particle emissions from a marine engine: chemical composition and aromatic emission profiles under various operating conditions. Environ. Sci. Technol. 48 (19), 11721–11729.

Takegawa, N., Miyakawa, T., Kawamura, K., Kondo, Y., 2007. Contribution of selected dicarboxylic and ω-oxocarboxylic acids in ambient aerosol to the m/z 44 signal of an aerodyne aerosol mass spectrometer. Aerosol Sci. Technol. 41 (4), 418–437.

Tree, D.R., Svensson, K.I., 2007. Soot processes in compression ignition engines. Prog. Energ. Combust. 33 (3), 272–309.

Tsai, J.-H., Chang, S.-Y., Chiang, H.-L., 2012. Volatile organic compounds from the exhaust of light-duty diesel vehicles. Atmos. Environ. 61, 499–506.

Wen, J., Wang, X., Zhang, Y., Zhu, H., Chen, Q., Tian, Y., Shi, X., Shi, G., Feng, Y., 2018.

PM2.5 source profiles and relative heavy metal risk of ship emissions: source samples from diverse ships, engines, and navigation processes. Atmos. Environ. 191, 55–63.
Wu, D., Li, Q., Ding, X., Sun, J., Li, D., Fu, H., Teich, M., Ye, X., Chen, J., 2018. Primary particulate matter emitted from heavy fuel and diesel oil combustion in a typical container ship: characteristics and toxicity. Environ. Sci. Technol. 52 (21), 12943–12951.
Wu, R.R., Xie, S.D., 2017. Spatial distribution of ozone formation in China derived from emissions of speciated volatile organic compounds. Environ. Sci. Technol. 51 (5), 2574–2583.
Xiao, Q., Li, M., Liu, H., Fu, M.L., Deng, F.Y., Lv, Z.F., Man, H.Y., Jin, X.X., Liu, S., He, K.B., 2018. Characteristics of marine shipping emissions at berth: profiles for particulate matter and volatile organic compounds. Atmos. Chem. Phys. 18 (13), 9527–9545.
Yao, Z.L., Shen, X.B., Ye, Y., Cao, X.Y., Jiang, X., Zhang, Y.Z., He, K.B., 2015. On-road emission characteristics of VOCs from diesel trucks in Beijing, China. Atmos. Environ. 103, 87–93.
Zhang, F., Chen, Y.J., Tian, C.G., Lou, D.M., Li, J., Zhang, G., Matthias, V., 2016. Emission factors for gaseous and particulate pollutants from offshore diesel engine vessels in China. Atmos. Chem. Phys. 16 (10), 6319–6334.
Zhang, Y., Wang, X., Blake, D.R., Li, L., Zhang, Z., Wang, S., Guo, H., Lee, F.S.C., Gao, B., Chan, L., Wu, D., Rowland, F.S., 2012. Aromatic hydrocarbons as ozone precursors before and after outbreak of the 2008 financial crisis in the Pearl River Delta region, south China. J. Geophys. Res. 117, 15306–15321.
Zhao, Y., Hennigan, C.J., May, A.A., Tkacik, D.S., de Gouw, J.A., Gilman, J.B., Kuster, W.C., Borbon, A., Robinson, A.L., 2014. Intermediate-volatility organic compounds: a large source of secondary organic aerosol. Environ. Sci. Technol. 48 (23), 13743–13750.